

From single-particle excitations to sound waves in a box-trapped atomic BEC

Samuel J. Garratt,^{1,2} Christoph Eigen,¹ Jinyi Zhang,¹ Patrik Turzák,¹
Raphael Lopes,^{1,3} Robert P. Smith,^{1,4} Zoran Hadzibabic,¹ and Nir Navon⁵

¹*Cavendish Laboratory, University of Cambridge, J. J. Thomson Avenue, Cambridge CB3 0HE, United Kingdom*

²*Theoretical Physics, University of Oxford, Parks Road, Oxford OX1 3PU, United Kingdom*

³*Laboratoire Kastler Brossel, Collège de France, CNRS, ENS-PSL University,
UPMC-Sorbonne Universités, 11 Place Marcelin Berthelot, F-75005 Paris, France*

⁴*Clarendon Laboratory, University of Oxford, Parks Road, Oxford OX1 3PU, United Kingdom*

⁵*Department of Physics, Yale University, New Haven, Connecticut 06520, USA*

We experimentally and theoretically investigate the lowest-lying axial excitation of an atomic Bose-Einstein condensate in a cylindrical box trap. By tuning the atomic density, we observe how the nature of the mode changes from a single-particle excitation (in the low-density limit) to a sound wave (in the high-density limit). We elucidate the physics of the crossover between the two limiting regimes using Bogoliubov theory, and find excellent agreement with the measurements. Finally, for large excitation amplitudes we observe a non-exponential decay of the mode, suggesting a nonlinear many-body decay mechanism.

I. INTRODUCTION

Low-energy excitations play a central role in our understanding of many-body systems. They characterise a system's low-temperature thermal properties, its response to small perturbations, and its near-equilibrium transport behaviour. The collective excitations of ultracold gases have been extensively studied in the traditional setting of a harmonic trap for bosons [1–7] and fermions [8–11] with contact interactions (including low-dimensional gases [12, 13]), as well as for Bose-Fermi mixtures [14], spin-orbit coupled gases [15], and gases with dipolar interactions [16, 17].

The recent developments in creating quasi-uniform box traps [18–21] have led to intriguing new possibilities. These traps provide a textbook setting for the study of short-wavelength excitations [22], but they also raise new questions on the nature of long-wavelength (system-size) collective modes, as highlighted by recent studies of sound propagation in 3D Bose [23] and Fermi [24] gases, and 2D Bose gases [25] (see also [26–28]). Due to the hard-wall boundary conditions the dynamics depend only on the interplay between kinetic and interaction energy; this is in stark contrast to harmonically trapped gases, where the lowest mode frequency is independent of interaction strength [29].

In this paper we experimentally and theoretically study the effect of interactions on the lowest-lying axial mode of a ^{87}Rb Bose-Einstein condensate (BEC) confined to a cylindrical box trap. This mode was previously exploited as a route to turbulence in a continuously driven Bose gas [23]. Here, we vary the atomic density by over two orders of magnitude to probe the near-equilibrium dynamics in both kinetic- and interaction-dominated regimes, and model our system using Bogoliubov theory to show how the mode evolves from a single-particle excitation to a sound wave. We conclude by studying the mode's decay and find that it is non-exponential, hinting at a nonlinear many-body decay mechanism.

II. RESONANT FREQUENCY

Our experiments start with the production of quasi-pure BECs of between $N = 0.9 \times 10^3$ and 137×10^3 ^{87}Rb atoms confined to a cylindrical optical box of length $L = 26(1)$ μm and radius $R = 16(1)$ μm (for details, see [18]). The experimental protocol used to probe the axial mode is shown schematically in Fig. 1(a). After creating the BEC we pulse an axial magnetic field gradient, corresponding to a potential difference $\Delta U = k_{\text{B}} \times 1$ nK over the box length, for a time

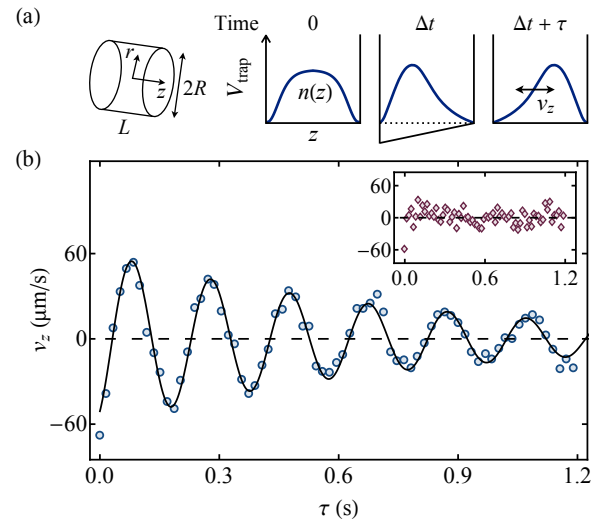


FIG. 1. Probing the lowest axial mode. (a) Illustration of the experimental protocol. We initially prepare a BEC of ^{87}Rb in a cylindrical box trap of length L and radius R . We then pulse a magnetic field gradient corresponding to $\Delta U = k_{\text{B}} \times 1$ nK along the box length for $\Delta t = 20$ ms. After a time τ of in-trap evolution we switch off the trap, and let the cloud evolve in free space for 140 ms before extracting its centre-of-mass, which reflects the velocity on release from the trap, v_z . (b) $v_z(\tau)$ for a BEC of $N = 13(1) \times 10^3$ atoms. We determine the oscillation frequency ω using a decaying sinusoidal fit. Inset: $v_z(\tau)$ for a non-condensed sample just above T_c , with $N = 10(1) \times 10^3$.

$\Delta t = 20$ ms, short compared to the period of the mode. We then hold the excited cloud in-trap for a variable time τ before switching off the trap and extracting the cloud's centre-of-mass (CoM) velocity in time-of-flight. We observe an oscillation of the cloud's velocity with τ , as shown in Fig. 1(b) for $N = 13(1) \times 10^3$ atoms.

If we repeat the same kick protocol with a thermal gas just above the condensation temperature, T_c , we see the same initial velocity as for a quasi-pure BEC. However, as shown in the inset of Fig. 1(b), there is no subsequent collective oscillation. For a classical gas to support hydrodynamic sound waves, local thermodynamic equilibrium needs to be established on timescales much shorter than the period of the wave [30]. With wavelength $2L$ and speed $\sim \sqrt{k_B T/m}$, where m is the atomic mass, this condition is $na^2 L \gg 1$; here a is the s -wave scattering length ($a \approx 100a_0$ for ^{87}Rb , where a_0 is the Bohr radius), $n = N/V$ the atomic number density and $V = \pi R^2 L$ the volume of the trap. For our thermal gases this condition would be fulfilled only for $N \gg 10^7$ atoms, so hydrodynamic sound waves cannot propagate even in our densest samples. The oscillations we observe in the condensed gas at high density correspond to Bogoliubov sound waves.

In Fig. 2 we summarise the measured condensate oscillation frequencies, and compare them with theories in different interaction regimes. Throughout the paper we model the trap as an infinitely deep cylindrical potential well.

At low density the gas is kinetic energy-dominated and we expect ideal gas behaviour. The system is then naturally described in terms of single-particle eigenstates α_j , which are separable in cylindrical coordinates (z, r, ϕ) . The BEC wavefunction is simply the single-particle ground state $\alpha_0 = \varphi(r) \cos(\pi z/L)$, with $\varphi(R) = 0$, and the lowest axial mode corresponds to $\alpha_1 = \varphi(r) \sin(2\pi z/L)$. The magnetic field gradient appears in the Hamiltonian as a perturbation $\hat{H}_{\text{kick}} = (\Delta U/L)\hat{z}$ for time Δt , and this preferentially excites particles from the condensate into α_1 . The excited state is then a superposition of α_0 and α_1 , which exhibits velocity oscillations at frequency

$$\omega_K = \frac{1}{\hbar}(\varepsilon_1 - \varepsilon_0) = \frac{3\hbar}{2m} \left(\frac{\pi}{L}\right)^2, \quad (1)$$

where ε_0 and ε_1 are the single-particle energies, and the subscript K denotes the kinetic-dominated regime. For our trap $\omega_K/(2\pi) = 2.5(2)$ Hz.

In the interaction-dominated regime the condensate wavefunction is uniform away from the walls, where it decays over the healing length $\xi \ll L$. The lowest axial mode is then a standing sound wave with wavelength $2L$ and speed of sound $(ng/m)^{1/2}$ [31], where $g = 4\pi\hbar^2 a/m$ is the strength of contact interactions. Consequently, at high density the axial mode frequency is

$$\omega_I = \left(\frac{gn}{m}\right)^{1/2} \frac{\pi}{L}. \quad (2)$$

Between these limiting regimes, we capture the crossover with a numerical solution to the Bogoliubov equations (see Section III B and [23]). In the next section we elucidate the physics of this crossover.

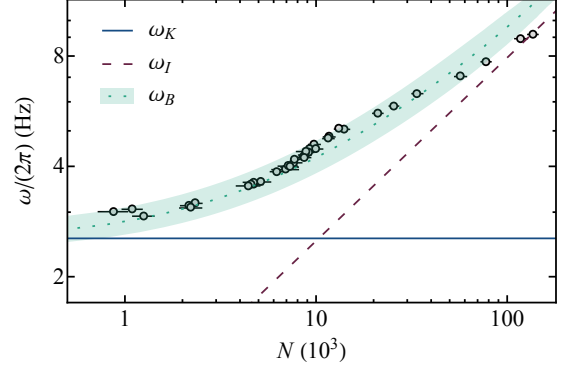


FIG. 2. Frequency of the lowest axial mode as a function of atom number, N . ω_K is the mode frequency in an ideal gas, and ω_I is the frequency of Bogoliubov sound with speed $(ng/m)^{1/2}$ and wavelength $2L$. These calculations use trap dimensions $L = 26$ μm and $R = 16$ μm . The shaded band ω_B shows the results of numerical Bogoliubov diagonalisation (see Section III B) accounting for the uncertainty of ± 1 μm in L and R .

III. CROSSOVER

Here we show how the condensate wavefunction of the interacting Bose gas, and its sound wave excitations, emerge from the single-particle eigenstates α_j . In second-quantised form, the Hamiltonian is

$$\hat{H} = \underbrace{\sum_j \varepsilon_j \hat{a}_j^\dagger \hat{a}_j}_{\hat{K}} + \underbrace{\frac{g}{2V} \sum_{ijkl} I_{ijkl}^\alpha a_i^\dagger \hat{a}_i^\dagger \hat{a}_j \hat{a}_l}_{\hat{I}}, \quad (3)$$

where \hat{K} and \hat{I} are the kinetic and interaction energy operators, respectively. \hat{a}_j^\dagger is the creation operator for single-particle eigenstate α_j , and $I_{ijkl}^\alpha = \int \alpha_i^* \alpha_j^* \alpha_k \alpha_l d^3r$, with wavefunctions normalised to unit volume.

A. Condensate

The non-interacting many-body ground state is $|\text{GS}\rangle = (\hat{a}_0^\dagger)^N |0\rangle / \sqrt{N!}$ where $|0\rangle$ is the vacuum of particles. Treating interactions perturbatively, the leading correction to the ground state, $|\delta\text{GS}\rangle$, comes from the operators of the form $\hat{a}_j^\dagger \hat{a}_0^\dagger \hat{a}_0 \hat{a}_0$. At first order

$$|\delta\text{GS}\rangle = \frac{g}{V} \sum_{j \neq 0} \frac{(N-1)\sqrt{N}}{\varepsilon_0 - \varepsilon_j} \frac{\hat{a}_j^\dagger \hat{a}_0}{\sqrt{N}} |\text{GS}\rangle, \quad (4)$$

where $\hat{a}_j^\dagger \hat{a}_0 |\text{GS}\rangle / \sqrt{N}$ is the many-body state with one atom excited to single-particle eigenstate α_j , and $(g/V)(N-1)\sqrt{N}$ is the transition matrix element between this many-body state and $|\text{GS}\rangle$. The correction, $\langle \delta\text{GS} | \delta\text{GS} \rangle$, is of order unity for $gn\sqrt{N} = \hbar\omega_K$, at which point perturbation theory fails. This occurs at much lower densities than one might expect from a simple comparison of interaction- and kinetic-energy scales;

that comparison would suggest that the perturbative regime extends up to $gn = \hbar\omega_K$. In our experiment, $gn\sqrt{N} = \hbar\omega_K$ for as few as 10^3 atoms.

In order to develop a physical intuition for the role of the $\hat{a}_j^\dagger \hat{a}_0^\dagger \hat{a}_0 \hat{a}_0$ operators, we contrast our system with a condensate with periodic boundary conditions. In the periodic case the condensate is spatially uniform regardless of interaction strength, and the terms involving $\hat{a}_j^\dagger \hat{a}_0^\dagger \hat{a}_0 \hat{a}_0$ operators vanish because α_j are momentum eigenstates. In our case these anomalous operators change the condensate shape. To show this explicitly we first write the interacting condensate wavefunction β_0 as a superposition of single-particle eigenstates

$$\beta_i = \sum_j U_{ij}(N) \alpha_j, \quad (5)$$

where U_{ij} is a unitary transformation with a parametric dependence on the interaction strength, in our case captured by N . We have also introduced the states $\beta_{i \neq 0}$ which are orthogonal to each other and to β_0 . We will see that, as N varies, β_0 follows a path in the space of single-particle wavefunctions along which nonperturbative corrections to the ground state vanish, and that this condition is equivalent to the Gross-Pitaevskii (GP) equation.

In the β basis \hat{K} is not diagonal, and we therefore have

$$\hat{H} = \sum_{ij} \langle \beta_i | \hat{K} | \beta_j \rangle \hat{b}_i^\dagger \hat{b}_j + \frac{g}{2V} \sum_{ijkl} I_{ijkl}^\beta \hat{b}_i^\dagger \hat{b}_j^\dagger \hat{b}_k \hat{b}_l, \quad (6)$$

where \hat{b}_i^\dagger is the creation operator for β_i , and I_{ijkl}^β are the corresponding overlap integrals. Assuming that the quantum depletion is small, the ground state has $\langle \hat{b}_0^\dagger \hat{b}_0 \rangle \gg \langle \hat{b}_i^\dagger \hat{b}_i \rangle$. In perturbation theory the dominant corrections to the ground state (as in Eq. (4)) then come from terms of the form

$$\langle \beta_i | \hat{K} | \beta_0 \rangle \hat{b}_i^\dagger \hat{b}_0 + \frac{g}{V} I_{i000}^\beta \hat{b}_i^\dagger \hat{b}_0^\dagger \hat{b}_0 \hat{b}_0, \quad (7)$$

in Eq. (6). The two terms in Eq. (7) give corrections with transition matrix elements scaling as $\hbar\omega_K \sqrt{N}$ and $gn\sqrt{N}$, respectively, and at the densities of interest they are nonperturbatively large; β_0 must therefore be chosen so that they cancel. Particle number conservation gives $\hat{b}_0^\dagger \hat{b}_0 = N - \sum_{i \neq 0} \hat{b}_i^\dagger \hat{b}_i$, and substituting this into the second term of Eq. (7) we see that the nonperturbative corrections vanish if

$$\int \beta_i^* \left(-\frac{\hbar^2}{2m} \nabla^2 + gn|\beta_0|^2 \right) \beta_0 d^3x = 0, \quad (8)$$

for all $i \neq 0$. Note that those terms in Eq. (7) which do not vanish under condition Eq. (8) can be treated perturbatively. Since the set of β_i are mutually orthogonal and form a complete basis, Eq. (8) implies

$$\left(-\frac{\hbar^2}{2m} \nabla^2 + gn|\beta_0|^2 \right) \beta_0 = \mu \beta_0, \quad (9)$$

for a constant μ , which is identified as the Hartree-Fock chemical potential. Eq. (9) is then the GP equation [31], which has

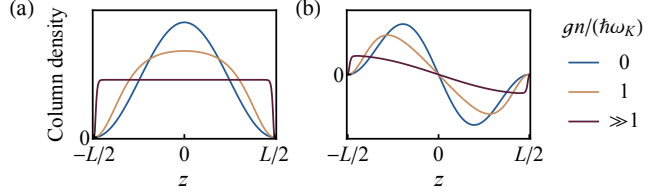


FIG. 3. (a) Axial density profile of the BEC, for three interaction strengths $gn/(\hbar\omega_K)$. (b) Change in the axial density profile due to the coherently-occupied axial mode, scaled by $\sqrt{\omega}$ so the amplitude for $gn/(\hbar\omega_K) \gg 1$ does not depend on N .

arisen from the sole assumption that one state, β_0 , has much greater occupation than those orthogonal to it. In practice we work with a finite set of single-particle eigenstates and compute β_0 by minimising the GP energy functional with respect to U_{0j} . This variational method ensures that Eq. (8) holds despite the finite basis size.

In Fig. 3(a) we illustrate how the condensate shape changes in the crossover between kinetic- and interaction-energy dominated regimes.

B. Excitations

To study the evolution of excitations with interaction strength we use Bogoliubov theory. Having determined β_0 variationally, we construct the set of $\beta_{i \neq 0}$ using the Gram-Schmidt procedure, then introduce the mean field $\hat{b}_0 = \sqrt{N}$ in Eq. (6). As in conventional Bogoliubov theory, we neglect terms cubic (and higher) in $\hat{b}_{i \neq 0}$ operators, thereby arriving at an effective quadratic Hamiltonian for the near-equilibrium dynamics. This is diagonalised using a bosonic transformation [32]

$$\hat{c}_i = \sum_j \left(P_{ij} \hat{b}_j + Q_{ij} \hat{b}_j^\dagger \right), \quad (10)$$

such that

$$\hat{H} \approx E_0 + \sum_j \hbar\omega_j \hat{c}_j^\dagger \hat{c}_j \equiv \hat{H}_B, \quad (11)$$

for appropriate P and Q . E_0 is the energy of the interacting ground state and \hat{c}_j^\dagger the creation operator for the j^{th} normal mode. Although the Gram-Schmidt procedure does not uniquely specify $\beta_{i \neq 0}$, P_{ij} and Q_{ij} adjust accordingly to uniquely specify \hat{c}_i .

In Fig. 3(b) we show how the axial density profile of the lowest-lying axial mode changes through the crossover. Note that the wavelength of the mode in the interaction-dominated regime is double of that in the ideal gas.

Before comparing our theoretical results with the experiments, it remains to be shown that throughout the crossover the axial kick \hat{H}_{kick} leads to velocity oscillations at the frequency of the lowest axial mode. Here we show that this is indeed the case, and that the excited state has a coherent occupation of normal modes. Approximating $\hat{b}_0 = \sqrt{N}$ and

assuming $N \gg 1$, we express \hat{H}_{kick} as a linear combination of normal mode operators

$$\begin{aligned}\hat{H}_{\text{kick}} &\approx \frac{\Delta U}{L} \sqrt{N} \sum_i \langle \beta_0 | \hat{z} | \beta_i \rangle \hat{b}_i + \text{h.c.}, \\ &= \frac{\Delta U}{L} \sqrt{N} \sum_j Z_j \hat{c}_j + \text{h.c.},\end{aligned}\quad (12)$$

where Z_j is given by the P and Q matrices [33] and h.c. denotes the Hermitian conjugate. We then treat \hat{H}_{kick} as a perturbation to \hat{H}_B and find the time-evolution operator in the interaction picture,

$$\hat{U}(\Delta t) = \prod_j \mathcal{T} \exp \left(-i \int_0^{\Delta t} (\eta_j e^{-i\omega_j t'} \hat{c}_j + \text{h.c.}) dt' \right), \quad (13)$$

where $\eta_j \equiv \Delta U \sqrt{N} Z_j / (\hbar L)$ and \mathcal{T} denotes time ordering. For the low energy modes $e^{-i\omega_j \Delta t} \approx 1$, so the time ordering operation is trivial. To obtain the state at the end of the kick we apply $\hat{U}(\Delta t)$ to the ground state of \hat{H}_B , $|\text{GS}\rangle_B$, which yields

$$|\eta\rangle \equiv \hat{U}(\Delta t) |\text{GS}\rangle_B = \prod_j e^{-|\eta_j \Delta t|^2/2} e^{-i\eta_j \Delta t \hat{c}_j^\dagger} |\text{GS}\rangle_B, \quad (14)$$

a coherent occupation of normal modes. Following the kick, the in-trap time evolution is generated by \hat{H}_B . To calculate the velocity of the cloud we first write the momentum operator in terms of the normal modes. Following the same procedure as in Eq. (12),

$$\hat{p}_z \approx \hbar \sqrt{N} \sum_j D_j \hat{c}_j + \text{h.c.}, \quad (15)$$

where $\hbar D_j$ is analogous to Z_j [34]. The axial velocity is then

$$\begin{aligned}\langle v_z(\tau) \rangle &= \frac{1}{Nm} \langle \eta | e^{i\hat{H}_B \tau / \hbar} \hat{p}_z e^{-i\hat{H}_B \tau / \hbar} | \eta \rangle \\ &= 2 \frac{\Delta t}{m} \frac{\Delta U}{L} \sum_j \text{Im} \left\{ D_j Z_j e^{-i\omega_j \tau} \right\}.\end{aligned}\quad (16)$$

The contribution of the j^{th} mode to the velocity amplitude therefore scales as $|Z_j D_j|$. We find numerically that the lowest axial mode contributes to over 80% of the amplitude over the whole range of N . This is in line with our single-mode interpretation of the observed oscillations (see Fig. 1(b)).

C. Truncated-basis models

To understand the effect of interactions on the axial mode frequency throughout the crossover, we calculate it using (progressively larger) truncated sets of low-energy single-particle eigenstates.

First, we consider just the two lowest single-particle eigenstates (the lowest even-parity state α_0 and the lowest odd-parity state α_1). In this case the condensate wavefunction is $\beta_0 = \alpha_0$, the mode involves only α_1 , and neither has the freedom to change its shape with increasing

$gn/(\hbar\omega_K)$. Here the bosonic transform in Eq. (10) gives $\hat{c}_1 = \cosh(\kappa) \hat{a}_1 + \sinh(\kappa) \hat{a}_1^\dagger$, where κ is chosen to diagonalise \hat{H}_B (see Eq. (11)). The resulting mode frequency is

$$\omega^{(2)} = \omega_K \sqrt{\left(1 + \frac{\mathcal{J}gn}{3\hbar\omega_K} \right)^2 - \left(\frac{2\mathcal{J}gn}{3\hbar\omega_K} \right)^2}, \quad (17)$$

where $\mathcal{J} \approx 2.10$ is the radial factor in the overlap integral I_{0011}^α . As shown in Fig. 4, this scheme fails to describe the dynamics even for values of $gn/(\hbar\omega_K)$ well below unity.

As a minimal model that does allow for the interaction-induced shape changes of both the condensate and the excitation mode, we consider a truncated set of the five lowest-energy α_j with zero angular momentum, and calculate the corresponding $\omega^{(5)}$. In this case β_0 is a superposition of three even-parity states, and the excited mode involves two of odd-parity; note that here we use five states because the third-lowest even state has a lower energy than the second-lowest odd one. We find that this simple model is sufficient to capture rather well most of the crossover, up to $gn/(\hbar\omega_K) \approx 3$ (see Fig. 4), where gn exceeds the maximum kinetic energy in the truncated set. For any $gn/(\hbar\omega_K)$ significantly larger than 3, the simple sound-wave calculation ω_I already provides a good approximation.

The agreement of the Bogoliubov calculations with the experimental data improves further as we consider ever larger basis sets, as shown by the 15-state calculation, $\omega^{(15)}$, in Fig. 4, and the full numerical result in Fig. 2; there ω_B was

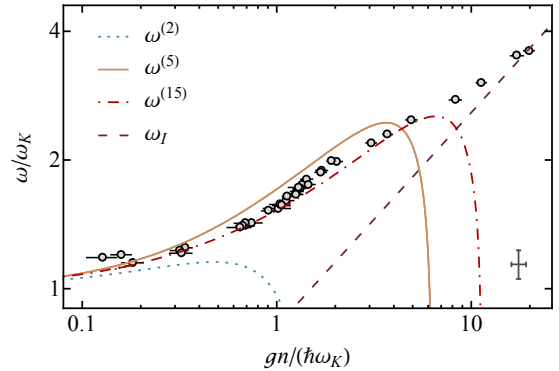


FIG. 4. Crossover from single-particle excitations to sound waves. We plot ω/ω_K as a function of the interaction strength, now parametrised by $gn/(\hbar\omega_K)$. Here we assume $L = 26 \mu\text{m}$ and $R = 16 \mu\text{m}$ for calculations. The grey x - y error bar (in the bottom right corner) indicates the fractional systematic uncertainties in the experimental data due to the uncertainties in the box dimensions. $\omega^{(2)}$ is determined using Bogoliubov theory within a truncated basis of just the two lowest-energy single-particle eigenstates of zero angular momentum (see text). This scheme fails even for relatively small $gn/(\hbar\omega_K)$, as it does not allow for the interaction-induced changes in the shape of the condensate or the excitation mode. $\omega^{(5)}$, based on a truncated basis of five single-particle eigenstates, is the minimal model that allows for the shape changes. This simple model already captures most of the crossover, and using progressively larger truncated bases does not qualitatively change the result, as shown by $\omega^{(15)}$, which is based on 15 single-particle eigenstates. ω_I is the sound-wave frequency, approached in the limit of large $gn/(\hbar\omega_K)$.

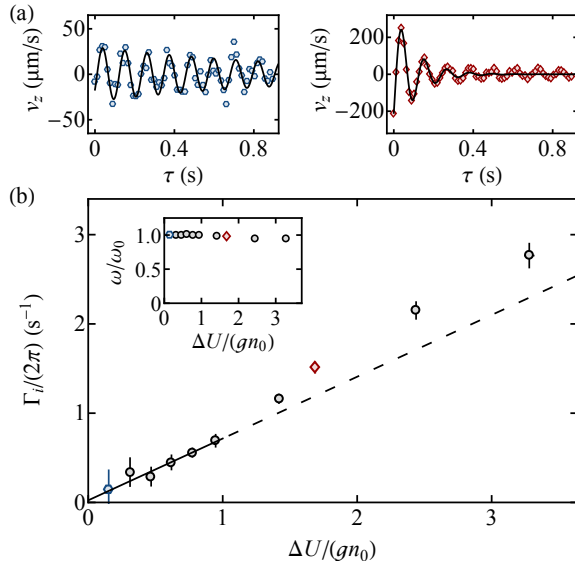


FIG. 5. Nonlinear damping of the lowest-lying axial mode in the interaction-dominated regime, with fixed density n_0 such that $gn_0 = k_B \times 2.1$ nK (corresponding to $gn_0/(\hbar\omega_K) \approx 17$). (a) Velocity oscillations following kicks with $\Delta U = k_B \times 0.3$ nK (left) and $k_B \times 3.6$ nK (right). The black lines show exponentially decaying sinusoidal functions obtained by fitting to the early-time data, $\tau < 0.25$ s. For large ΔU (right panel) the decay is clearly non-exponential. (b) Initial decay rate Γ_i as a function of the normalized kick amplitude $\Delta U/(gn_0)$. The black line is a linear fit to data with $\Delta U/(gn_0) < 1$. Inset: frequency of the damped oscillation ω normalized to the low- ΔU value, ω_0 .

calculated using $\sim 10^2$ single-particle states with kinetic energies up to $\approx 60 \hbar\omega_K$. However, the success of the simple $\omega^{(5)}$ calculation highlights the key qualitative message: most of the physics of the crossover is captured by including, at lowest order, the interaction-induced shape changes that arise due to the experimentally relevant fixed boundary conditions.

IV. BEYOND LINEAR RESPONSE

We have so far neglected any coupling between the normal modes of the BEC. However, we observe at least a weak damping in all the frequency measurements summarised in Figs. 2 and 4; see for instance Fig. 1(b). In general, the nonzero temperature of our gases will lead to Landau damping [35], but our conservative upper bound of $T < 10$ nK suggests a decay rate of $\Gamma_{\text{Landau}}/(2\pi) < 0.2$ s $^{-1}$, much smaller than observed.

Here we examine this damping for different kick amplitudes, focusing on the interaction-dominated regime, with $gn/(\hbar\omega_K) \approx 17$; we fix gn to $gn_0 = k_B \times 2.1(2)$ nK (by fix-

ing the atom number to $N = 1.2(1) \times 10^5$), and vary the kick amplitude ΔU . Fig. 5(a) shows $v_z(\tau)$ following kicks with $\Delta U = k_B \times 0.3$ nK (left panel) and $k_B \times 3.6$ nK (right panel). For the weak kick only a subtle damping is observed, and an exponentially decaying sine (black line), fit to the early-time data ($\tau < 0.25$ s), captures the data well for all τ . However, for the stronger kick we clearly see a rapid initial decay followed by a long-lived oscillation. This is accentuated by the same early-time fit (black line), which clearly fails to capture the data for $\tau \gtrsim 0.4$ s.

We characterise the damping using the initial velocity-decay rate, Γ_i , extracted from the early-time ($\tau < 0.25$ s) fits. In Fig. 5(b) we show Γ_i versus normalised kick amplitude, $\Delta U/(gn_0)$, and in the inset we show that the mode frequency is approximately constant across our whole range of ΔU . At least for relatively weak kicks ($\Delta U \lesssim gn_0$) the damping rate appears to be linear in the kick amplitude, essentially vanishing (within experimental errors) as $\Delta U \rightarrow 0$. Both the clearly non-exponential decay, and the dependence of Γ_i on ΔU , point towards a nonlinear many-body decay mechanism.

V. CONCLUSIONS AND OUTLOOK

We have measured the dynamics of an atomic BEC in a cylindrical box trap following an axial kick, thereby probing its lowest axial mode. By tuning the gas density we studied the evolution from single-particle to many-body dynamics. We used a simple model to elucidate the effect of interactions, and numerically evaluated the mode frequency over the whole range of densities, finding excellent agreement with the experiments. Going beyond linear response in the interaction-dominated regime, we observed a non-exponential decay of the excitation, hinting at a nonlinear many-body decay mechanism. A future challenge is to understand this decay mechanism, and in particular its dependence on the interaction strength.

VI. ACKNOWLEDGEMENTS

We are grateful to F. Werner and J. T. Chalker for comments on the manuscript. This work was supported by EPSRC [Grants No. EP/N011759/1 and No. EP/P009565/1], ERC (QBox), AFOSR, and ARO. N.N. acknowledges support from Trinity College (Cambridge) and the David and Lucile Packard Foundation. R.L. acknowledges support from the E.U. Marie-Curie program [Grant No. MSCA-IF-2015 704832] and Churchill College, Cambridge. R.P.S. acknowledges support from the Royal Society.

[1] D. S. Jin, J. R. Ensher, M. R. Matthews, C. E. Wieman, and E. A. Cornell, “Collective Excitations of a Bose-Einstein Con-

densate in a Dilute Gas,” *Phys. Rev. Lett.* **77**, 420 (1996).

[2] M. O. Mewes, M. R. Andrews, N. J. van Druten, D. M. Kurn, D. S. Durfee, C. G. Townsend, and W. Ketterle, “Collective Excitations of a Bose-Einstein Condensate in a Magnetic Trap,” *Phys. Rev. Lett.* **77**, 988 (1996).

[3] M. R. Andrews, D. M. Kurn, H.-J. Miesner, D. S. Durfee, C. G. Townsend, S. Inouye, and W. Ketterle, “Propagation of Sound in a Bose-Einstein Condensate,” *Phys. Rev. Lett.* **79**, 553 (1997).

[4] O. M. Maragò, S. A. Hopkins, J. Arlt, E. Hodby, G. Hechenblaikner, and C. J. Foot, “Observation of the Scissors Mode and Evidence for Superfluidity of a Trapped Bose-Einstein Condensed Gas,” *Phys. Rev. Lett.* **84**, 2056 (2000).

[5] J. Steinhauer, R. Ozeri, N. Katz, and N. Davidson, “Excitation Spectrum of a Bose-Einstein Condensate,” *Phys. Rev. Lett.* **88**, 120407 (2002).

[6] R. Meppelink, S. B. Koller, and P. van der Straten, “Sound propagation in a Bose-Einstein condensate at finite temperatures,” *Phys. Rev. A* **80**, 043605 (2009).

[7] D. S. Lobser, A. E. S. Barentine, E. A. Cornell, and H. J. Lewandowski, “Observation of a persistent non-equilibrium state in cold atoms,” *Nat. Phys.* **11**, 1009 (2015).

[8] M. Bartenstein, A. Altmeyer, S. Riedl, S. Jochim, C. Chin, J. Hecker Denschlag, and R. Grimm, “Collective Excitations of a Degenerate Gas at the BEC-BCS Crossover,” *Phys. Rev. Lett.* **92**, 203201 (2004).

[9] J. Joseph, B. Clancy, L. Luo, J. Kinast, A. Turlapov, and J. E. Thomas, “Measurement of Sound Velocity in a Fermi Gas near a Feshbach Resonance,” *Phys. Rev. Lett.* **98**, 170401 (2007).

[10] S. Nascimbène, N. Navon, K. J. Jiang, L. Tarruell, M. Teichmann, J. McKeever, F. Chevy, and C. Salomon, “Collective Oscillations of an Imbalanced Fermi Gas: Axial Compression Modes and Polaron Effective Mass,” *Phys. Rev. Lett.* **103**, 170402 (2009).

[11] L. A. Sidorenkov, M. K. Tey, R. Grimm, Y.-H. Hou, L. Pitaevskii, and S. Stringari, “Second sound and the superfluid fraction in a Fermi gas with resonant interactions,” *Nature* **498**, 78 (2013).

[12] H. Moritz, T. Stöferle, M. Köhl, and T. Esslinger, “Exciting Collective Oscillations in a Trapped 1D Gas,” *Phys. Rev. Lett.* **91**, 250402 (2003).

[13] E. Vogt, M. Feld, B. Fröhlich, D. Pertot, M. Koschorreck, and M. Köhl, “Scale Invariance and Viscosity of a Two-Dimensional Fermi Gas,” *Phys. Rev. Lett.* **108**, 070404 (2012).

[14] I. Ferrier-Barbut, M. Delehaye, S. Laurent, A. T. Grier, M. Pierce, B. S. Rem, F. Chevy, and C. Salomon, “A mixture of Bose and Fermi superfluids,” *Science* **345**, 1035 (2014).

[15] J.-Y. Zhang, S.-C. Ji, Z. Chen, L. Zhang, Z.-D. Du, B. Yan, G.-S. Pan, B. Zhao, Y.-J. Deng, H. Zhai, S. Chen, and J.-W. Pan, “Collective Dipole Oscillations of a Spin-Orbit Coupled Bose-Einstein Condensate,” *Phys. Rev. Lett.* **109**, 115301 (2012).

[16] G. Bismut, B. Pasquiou, E. Maréchal, P. Pedri, L. Vernac, O. Gorceix, and B. Laburthe-Tolra, “Collective Excitations of a Dipolar Bose-Einstein Condensate,” *Phys. Rev. Lett.* **105**, 040404 (2010).

[17] L. Chomaz, R. M. W. van Bijnen, D. Petter, G. Faraoni, S. Baier, J. H. Becher, M. J. Mark, F. Wächtler, L. Santos, and F. Ferlaino, “Observation of roton mode population in a dipolar quantum gas,” *Nat. Phys.* **14**, 442 (2018).

[18] A. L. Gaunt, T. F. Schmidutz, I. Gotlibovych, R. P. Smith, and Z. Hadzibabic, “Bose-Einstein Condensation of Atoms in a Uniform Potential,” *Phys. Rev. Lett.* **110**, 200406 (2013).

[19] L. Chomaz, L. Corman, T. Bienaimé, R. Desbuquois, C. Weitenberg, S. Nascimbène, J. Beugnon, and J. Dalibard, “Emergence of coherence via transverse condensation in a uniform quasi-two-dimensional Bose gas,” *Nat. Commun.* **6**, 6162 (2015).

[20] B. Mukherjee, Z. Yan, P. B. Patel, Z. Hadzibabic, T. Yefsah, J. Struck, and M. W. Zwierlein, “Homogeneous Atomic Fermi Gases,” *Phys. Rev. Lett.* **118**, 123401 (2017).

[21] K. Hueck, C. Luick, L. Sobirey, J. Siegl, T. Lompe, and H. Moritz, “Two-Dimensional Homogeneous Fermi Gases,” *Phys. Rev. Lett.* **120**, 060402 (2018).

[22] R. Lopes, C. Eigen, A. Barker, K. G. H. Viebahn, M. Robert-de Saint-Vincent, N. Navon, Z. Hadzibabic, and R. P. Smith, “Quasiparticle energy in a strongly interacting homogeneous Bose-Einstein condensate,” *Phys. Rev. Lett.* **118**, 210401 (2017).

[23] N. Navon, A. L. Gaunt, R. P. Smith, and Z. Hadzibabic, “Emergence of a turbulent cascade in a quantum gas,” *Nature* **539**, 72 (2016).

[24] M. Zwierlein, private communication.

[25] J. L. Ville, R. Saint-Jalm, É. Le Cerf, M. Aidelsburger, S. Nascimbène, J. Dalibard, and J. Beugnon, “Sound Propagation in a Uniform Superfluid Two-Dimensional Bose Gas,” *Phys. Rev. Lett.* **121**, 145301 (2018).

[26] M. Ota and S. Stringari, “Second sound in a two-dimensional Bose gas: From the weakly to the strongly interacting regime,” *Phys. Rev. A* **97**, 033604 (2018).

[27] M. Ota, F. Larcher, F. Dalfovo, L. Pitaevskii, N. P. Proukakis, and S. Stringari, “Collisionless Sound in a Uniform Two-Dimensional Bose Gas,” *Phys. Rev. Lett.* **121**, 145302 (2018).

[28] A. Cappellaro, F. Toigo, and L. Salasnich, “Collisionless Dynamics in Two-Dimensional Bosonic Gases,” *Phys. Rev. A* **98**, 043605 (2018).

[29] W. Kohn, “Cyclotron Resonance and de Haas-van Alphen Oscillations of an Interacting Electron Gas,” *Phys. Rev.* **123**, 1242 (1961).

[30] P. M. Chaikin and T. C. Lubensky, *Principles of Condensed Matter Physics* (Cambridge University Press, 1995).

[31] L. Pitaevskii and S. Stringari, *Bose-Einstein Condensation and Superfluidity* (Oxford University Press, 2016).

[32] J.-P. Blaizot and G. Ripka, *Quantum Theory of Finite Systems*, Vol. 3 (MIT Press, 1986).

[33] Defining the inverse matrices P^{-1} and Q^{-1} via $\hat{b}_i = \sum_j [P_{ij}^{-1} \hat{c}_j + Q_{ij}^{-1} \hat{c}_j^\dagger]$, we have $Z_j = \sum_i [\langle \beta_0 | \hat{z} | \beta_j \rangle P_{ij}^{-1} + \langle \beta_j | \hat{z} | \beta_0 \rangle (Q_{ij}^{-1})^*]$.

[34] Using the inverse matrices P^{-1} and Q^{-1} , we have $\hbar D_j = \sum_i [\langle \beta_0 | \hat{p}_z | \beta_j \rangle P_{ij}^{-1} + \langle \beta_j | \hat{p}_z | \beta_0 \rangle (Q_{ij}^{-1})^*]$.

[35] L. P. Pitaevskii and S. Stringari, “Landau damping in dilute Bose gases,” *Phys. Lett. A* **235**, 398 (1997).